Parasitology Research (2019) 118:1137–1146
https://doi.org/10.1007/s00436-019-06244-7

FISH PARASITOLOGY - ORIGINAL PAPER

Description of *Myxobolus xiantaoensis* n. sp. from the fins of yellow catfish in China: a species previously attributed to *Myxobolus physophilus* Reuss, 1906 in Chinese records

Urfa Bin Tahir[1,2] · QingXiang Guo[1,2] · DanDan Zhao[1,2] · Yang Liu[1,2] · Zemao Gu[1,2]

Received: 8 June 2018 / Accepted: 31 January 2019 / Published online: 5 March 2019

Abstract
Myxozoans are economically important cnidarian endoparasites. Members of this group have been traditionally characterized by a morphology-based taxonomic system. Because myxozoans possess few morphological characters, these data are routinely accompanied by biological traits (host/organ/tissue specificity) and molecular data when describing or identifying myxozoan species. In the present study, a species of *Myxobolus* was collected from the fins of yellow catfish *Tachysurus fulvidraco* Richardson, 1846, which was consistent in spore morphology and host/organ specificity with Chinese records of *Myxobolus physophilus* Reuss, 1906. However, these earlier records and our own findings are inconsistent with the original description of *M. physophilus* from Russia. Specifically, there are differences in spore morphology (shape, intercapsular appendix, and polar capsule size), the infection site (air bladder vs. fins), and the host affinity (common rudd vs. yellow catfish). The inconsistencies allow us to conclude that both the present *Myxobolus* species and Chinese records of *M. physophilus* are distinct from the original description of *M. physophilus* and represent a new *Myxobolus* species, which we named *Myxobolus xiantaoensis* n. sp.

Keywords Myxozoan · *Myxobolus physophilus* · *Myxobolus xiantaoensis* n. sp., · *Tachysurus fulvidraco* · SSU rDNA · Taxonomic confusion

Introduction

Myxozoans are widespread and economically important cnidarian parasites; they are well known for their infections of fish (Abdel-Ghaffar et al. 2005; Székely and Molnár 1999). Within the myxozoans, *Myxobolus* Bütschli, 1882 is the most speciose genus, comprising more than 900 known species worldwide (Eiras et al. 2005, 2014; Liu et al. 2014; Lom and Dyková 2006; Naldoni et al. 2015; Székely et al. 2015). Most of these species have been traditionally defined using morphological and biological traits (host/organ specificity and tissue tropism) to resolve taxonomic conflicts (Molnár 1994, 2002; Molnár et al. 2009; Székely et al. 2015; Liu et al. 2016). Since the beginning of the twenty-first century, the molecular marker (mainly the small subunit ribosomal DNA) has been used extensively to provide a more comprehensive strategy to discriminate between morphologically complex species (Székely et al. 2015; Okamura et al. 2015). Thus, the use of three approaches in combination (morphology, biological traits, and molecular markers) have yielded a well-accepted holistic framework for myxozoan classification (Atkinson et al. 2015; Fiala et al. 2015; Forró and Eszterbauer 2016; Heiniger and Adlard 2013).

Yellow catfish *Tachysurus fulvidraco* is a freshwater fish mostly distributed in East and Southeast Asia (Liu 1997). In China, its annual output has increased by 356 million kg (Yuan and Zhao 2016). Given the importance of this host species, it has been examined for parasites, and 23 myxozoan

Section Editor: Christopher Whipps

✉ Zemao Gu
guzemao@mail.hzau.edu.cn

[1] Department of Aquatic Animal Medicine, College of Fisheries, Huazhong Agricultural University, Wuhan, People's Republic of China

[2] Hubei Engineering Technology Research Center for Aquatic Animal Diseases Control and Prevention, Wuhan, People's Republic of China

species have been described based on their different infection sites (Chen and Ma 1998). Few of these descriptions have corresponding molecular data.

Herein, as part of a continuing study of freshwater myxozoans biodiversity, a *Myxobolus* species was sampled from the fins of yellow catfish. The spore morphology, host affinity, and organ affected by this *Myxobolus* species were similar to those of *Myxobolus physophilus* previously recorded in China (Chen 1973; Chen and Ma 1998). However, *M. physophilus* was originally reported in Russia from the air bladder of common rudd *Scardinius erythrophthalmus* Linnaeus, 1758 (Reuss 1906). Later, a *Myxobolus* species in China was attributed to *M. physophilus* from the fins and urinary bladder of *T. fulvidraco* based on morphological classification (Chen 1973). Subsequently, Chen and Ma (1998) recorded the same species from multi-infection sites of extensively distributed multi-fish hosts, including the gills of *Abbottina rivularis* Basilewsky, 1855, the kidney and urinary bladder of *Tachysurus nitidus* Sauvage and Dabry de Thiersant, 1874, and the gills, kidney, and fins of *T. fulvidraco* and *Sarcocheilichthys sinensis* Bleeker, 1871.

Taking in to account the usually strict tissue specificity of myxozoans (Molnár 1994, 2002; Molnár and Eszterbauer 2015), it would be unexpected for a single species to be reported in multi-infection sites of multi-fish hosts as reported previously (Chen 1973; Chen and Ma 1998). To resolve existing uncertainties in the Chinese records of *M. physophilus* (Chen 1973; Chen and Ma 1998), the newly collected material was characterized considering a combination of three approaches (morphological characteristics, biological traits, and DNA sequence data) for myxozoan species identification.

Materials and methods

Host sampling and morphological analysis

Yellow catfish *Tachysurus fulvidraco* were collected using a fine-meshed seine from the fish pond in Xiantao, Hubei, China, in April 2016 ($n = 50$; total length 16–33 cm; weight 41–73 g). Specimens were transported alive to the Department of Aquatic Animal Medicine, College of Fisheries, Huazhong Agricultural University, Wuhan, Hubei, China, and held in aquaria prior to being euthanized with an overdose of MS-222 (Sigma-Aldrich, Co., Ltd., St. Louis, MO., USA). Standard techniques were utilized for myxosporean examination within 24 h of transportation (Lom and Dykovà 1992).

Macroscopic inspection (external and internal) was conducted for the detection of visible myxozoan cysts. For microscopic examination, squash samples were prepared from various vital organs, including the gills, skin, intestine, kidney, spleen, liver, gallbladder, and urinary bladder. For parasitological examinations, fresh smears were visualized and photographed by a BX53 Olympus light microscope (Nomarski differential interference contrast) equipped with an Olympus DP73 digital camera, using CellSens software (Olympus, Hamburg, Germany). Myxospores (50 data points for each dimension) were measured by means of digitized images using Adobe Photoshop CC software (Adobe Systems, San Jose, CA, USA). Mean and standard deviations of fresh myxospore dimensions were calculated. Line drawings were drawn with the guide of digitized images using Adobe Photoshop CC software.

Histopathological examination

Biopsies of infected tissue were fixed in Bouin's solution, gradient-dehydrated, embedded in paraffin wax, sectioned at 4–6 μm and stained with hematoxylin and eosin (H & E). Slides were viewed and photographed by the abovementioned microscope.

DNA extraction, amplification, and sequencing

The squash samples were prepared from fresh samples of three different infected fish and centrifuged at 10,000×*g* for 5 min. Genomic DNA was extracted from pelleted myxospores using the TIANamp Genomic DNA Kit (TIANGEN Biotech, Beijing, China). The SSU rDNA sequence was amplified by polymerase chain reaction (PCR) using 18e (Hillis and Dixon 1991) and 18R (Whipps et al. 2003) primer pairs in a 50-μl reaction mixture, containing 25 μl 2× PrimeSTAR® Max Premix (Takara, Dalian, China), 2 μl of each primer, 17 μl distilled water, and approximately 150–200 ng of genomic DNA. The PrimeSTAR® Max DNA Polymerase (Takara, Dalian, China) was used to ensure a high-fidelity sequence. Amplification conditions included an initial denaturation at 98 °C for 5 min, followed by 35 cycles at 98 °C for 10 s, 55 °C for 15 s, 72 °C for 1 min, and a final extension at 72 °C for 3 min. The PCR products were electrophoresed through 1% agarose gels, purified using a Universal DNA Purification Kit (TIANGEN Biotech, Beijing, China) and cloned into the pMD19-T vector system (Takara, Dalian, China). Before cloning in the pMD19-T vector, A-tailing was performed in a 20-μl reaction mixture comprised of 14.5 μl amplified product, 3 μl deoxyribonucleotide triphosphates (dNTPs), 2 μl Taq Buffer, and 0.5 μl Taq DNA Polymerase (CWBIO, Beijing, China) at 72 °C for 20 min. Inserts from three positive clones were sequenced with an ABI PRISM® 3730XL DNA sequencer (Applied Biosystems Inc., Foster, USA) using M13F, M13R, and middle primer 5W1F 5′-GACAAATCACTTCACGAAC-3′.

Phylogenetic analyses

The obtained contiguous sequences were determined to have originated from a myxozoan (*Myxobolus*) by BLAST search. To explore the phylogenetic relationship of the isolated species, 35 sequences consisted of BLAST hits and prior phylogenies were retrieved from the NCBI nucleotide database. *Ceratonova shasta* was used as an out-group taxon. The dataset was aligned in MAFFT 7.271 (Katoh and Standley 2013) and corrected manually using a sequence alignment editor program BioEdit (Hall 1999). The putative gaps or ambiguous regions were deleted to ensure the comparison of homologous positions. Phylogenetic analyses were conducted by the Bayesian inference (BI) and maximum likelihood (ML) methods. The best evolutionary model of nucleotide substitution for the ML and BI analyses was determined by MrModeltest v. 2.3 (Nylander 2004), which identified the optimal evolutionary model as the general time reversible model (GTR + I + G) using the Akaike information criteria (AIC). ML analysis was conducted using PhyML v. 3.0 (Guindon et al. 2010). Nucleotide frequencies were determined (A = 0.2677, C = 0.1890, G = 0.2679, T = 0.2754) and the six rates of nucleotide substitution were calculated as AC = 0.8674, AG = 3.2432, AT = 1.7124, CG = 0.6639, CT = 4.9663, and GT = 1.0000. The proportion of invariable sites was 0.2880, and the alpha value of the gamma distribution parameter was 0.4060. Bootstrap confidence values were calculated with 1000 replicates. Bayesian analysis was performed in MrBayes v. 3.1 (Ronquist and Huelsenbeck 2003) by means of the above evolutionary model, with 1×10^6 generations and tree samples per 100 generations and a burn-in of 2500 trees. The resulting topologies were annotated with MEGA v. 6.06 software package (Tamura et al. 2013).

Results

Of the 50 yellow catfish specimens, 3 (6%) were found bearing pinkish flower-like aggregates of cysts and tended to exist at the tips of fins (Fig. 1). Approximately 18–30 cysts per infected fish were observed. After rupturing the cysts, mature myxospores with two unequal polar capsules were observed, morphologically consistent with a *Myxobolus* species. This *Myxobolus* species was considered to be conspecific with Chinese records of *Myxobolus physophilus* (Figs. 2 and 3, Table 1). However, both our species and the previous records from China are inconsistent with the original description of *M. physophilus* (Figs. 2 and 3, Table 1). As we propose a new species, *Myxobolus xiantaoensis* n. sp., to account for our observations and to replace previous records of *M. physophilus* from China.

Family Myxobolidae Thélohan, 1892

Genus *Myxobolus* Bütschli, 1882

Myxobolus xiantaoensis n. sp.

Type host: Yellow catfish *Tachysurus fulvidraco* (Siluriformes: Bagridae).

Local name of the host: Huang Sang Yu.

Type locality: Fish pond in Xiantao, Hubei, (30° 22′ N, 113° 27′E) China.

The site of infection: Surface of fin hemisegments.

Date of sampling: 25 April 2016.

Prevalence: 3/50 (6%).

Voucher material: 5% formalin fixed mature spores deposited in National Zoological Museum of China, Institute of Zoology, Chinese Academy of Sciences (accession number 2016042501), and Department of Aquatic Animal Medicine, College of Fisheries, Huazhong Agricultural University, Wuhan, the People's Republic of China (accession number CF2016042502).

Representative DNA sequence: The SSU rDNA sequence was deposited into GenBank under the accession number KY421105.

Etymology: This specific epithet is proposed after the type locality, Xiantao city.

Morphological description

Myxospores were pyriform in the frontal view (Figs. 2a, b, and 3a, b), biconvex in sutural view (Figs. 2c, d, and 3c, d), pointed anteriorly, and rounded posteriorly, measuring 12.6 ± 0.6 (11.3–13.9) μm long, 9.6 ± 0.6 (8.4–11.1) μm wide, and 7.1 ± 0.4 (6.1–7.7) μm thick. A transparent mucous envelope was occasionally observed in the posterior end of a few myxospores (Fig. 2b, d). Two unequally sized and eggplant-shaped polar capsules were present in the apical part of the myxospore. The larger polar capsule was 6.83 ± 0.5 (6.0–8.1) μm long and 3.4 ± 0.2 (3.0–3.8) μm wide, while the smaller one was 6.4 ± 0.3 (5.5–7.4) μm in length and 3.6 ± 0.2 (3.2–3.9) μm in width. Inside the polar capsules, polar filaments were coiled by 6–8 turns. The intracapsular appendix was almost 1/6th of the total length of spore (Figs. 2 and 3a–d). Sporoplasm nuclei and iodinophilous vacuoles were not prominent.

Histopathology

Histological examination showed that cysts developed under the epidermis, on the surface of hemisegments (Figs. 4a, e, f, g). Many small plasmodia were joined together to produce a large cyst covered by a relatively thick connective tissue capsule (Fig. 4). A number of alarming cells (club cells or leydig cells), mucus cells, and mononuclear cells were observed in the

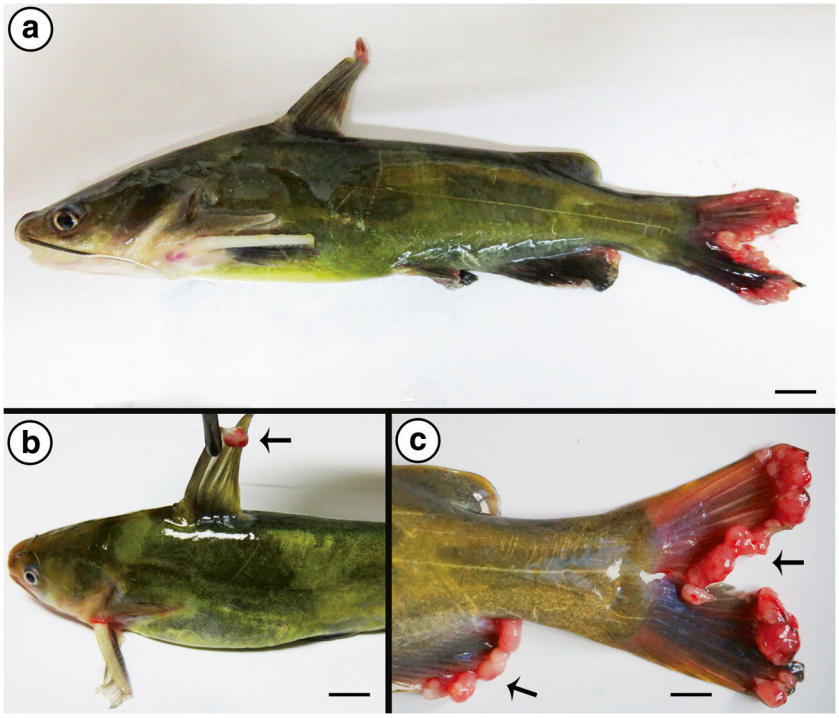

Fig. 1 Gross appearance of the affected yellow catfish fish *T. fulvidraco* showing the extensive nature of the lesion. **a**–**c** Flower-like appearance of the cysts on the border of the fins (arrow). Scale bar: 1 cm

epidermis of fins (Fig. 4b–d). *M. xiantaoensis* n. sp. markedly deforms the cartilaginous substance of the fin-rays (Fig. 4a, e, f–h). Moreover, the developing cysts substantially change the structure of the hemisegments of fin-ray (Fig. 4e). Within the developing cysts, the cartilage can be found, as small cartilaginous islets, in the cysts capsule (Figs. 4a).

Molecular data

A 1990-bp-long SSU rDNA sequence (GenBank KY421105) was generated for the present *Myxobolus* species. Based on GenBank BLAST analysis, the SSU rDNA sequence of the present isolates was most similar to those of *Myxobolus pseudowulii* (94.0% sequence identity; 100% coverage; KY229918), *Myxobolus voremkhai* (91.0% sequence identity; 100% coverage; KY229919), and *Myxobolus branchicola* (90.0% sequence identity; 100% coverage; JN616264). The ML and BI analyses produced similar tree topologies, although with slightly different support values at the branch nodes (Fig. 5). In the light of the result of the phylogenetic analysis, species clustered in three clades: clade I consisted of *Myxobolus*, *Unicauda*, *Henneguya*, and *Thelohanellus* species; clade II consisted of *Myxobolus*, and *Henneguya* species; and clade III consisted of the species of genus *Myxobolus* (Fig. 5). *M. xiantaoensis* n. sp. was sister to *M. pseudowulii* in clade I that included the myxozoan species infecting the Siluriformes fishes from China, Malaysia, and the USA (Fig. 5).

Remarks

Comparative analyses (morphometric data, biological traits, and images) of species infecting the fins of Siluriformes (including yellow catfish from China) showed that in addition to *M. physophilus*, the four other *Myxobolus* species recorded by Chen and Ma (1998) (*Myxobolus aureatus* Ward, 1919, *Myxobolus oviformis* Thélohan, 1892, *Myxobolus ochowensis* Chen in Chen & Ma, 1998, and *Myxobolus huamaensis* Liu 2014) also had overlapping features with *M. xiantaoensis* n. sp. (Table 1). Although all these descriptions lacked molecular data, *M. xiantaoensis* n. sp. clearly showed a unique morphology, in terms of the spore shape and size, and lesions, which were flower-like. Notably, *M. xiantaoensis* n. sp. and its conspecific Chinese records were clearly differed from the original description of *M. physophilus* in spore shape (Fig. 3) and biological traits (Table 1). It is difficult to compare the real tissue specificity of *M. xiantaoensis* n. sp. and *M. physophilus* because the original description does not offer a detailed reference to the tissue in which parasite development occurred.

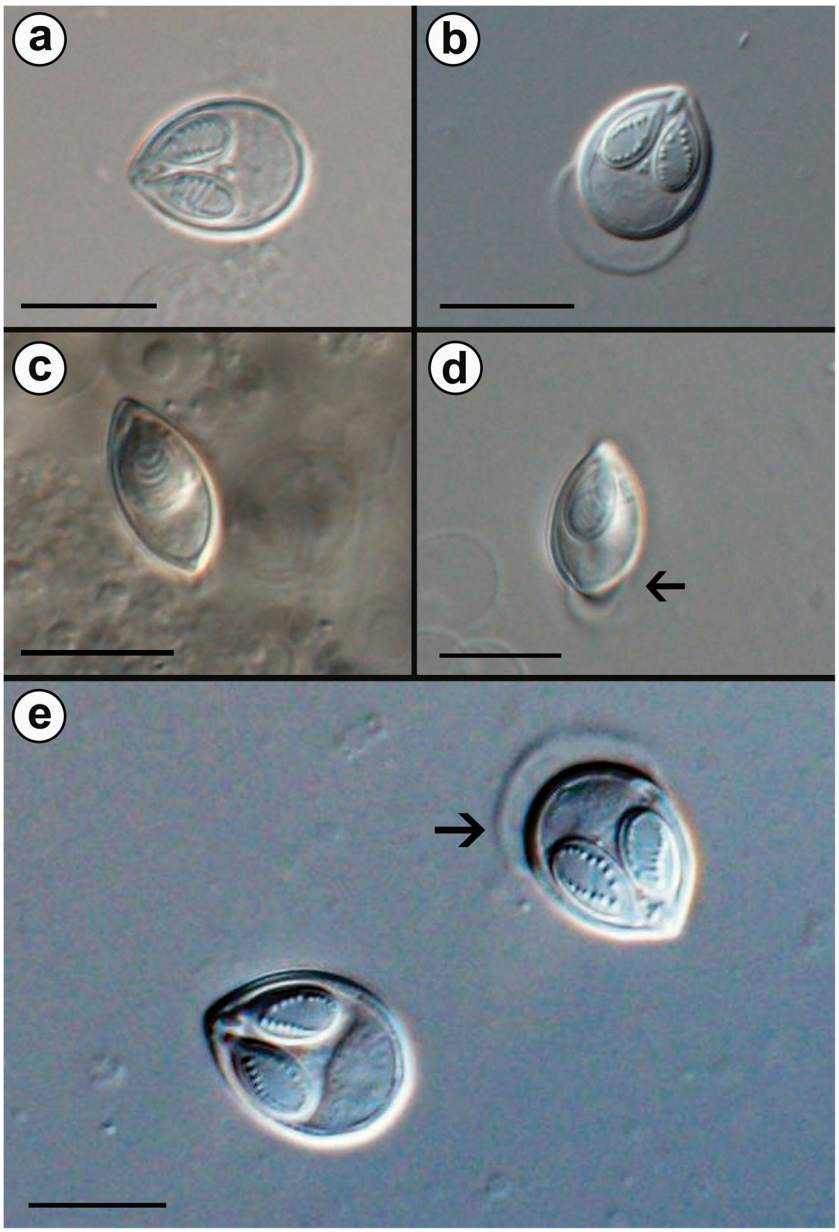

Fig. 2 Photomicrographs of fresh spores of *M. xiantaoensis* n. sp. **a** Frontal view without mucous envelope. Scale bar: 10 μm. **b** Frontal view with the mucous envelope. Scale bar: 10 μm. **c** Sutural view without the mucous envelope. Scale bar: 10 μm. **d** Sutural view with the mucous envelope. Scale bar: 10 μm. **e** *M. xiantaoensis* n. sp. with and without mucous envelope. Scale bar: 10 μm

Discussion

To facilitate myxozoan species identification, spores were collected from cysts present on the fins of yellow catfish and studied by morphological, biological, and molecular methods. A holistic comparison of the present *Myxobolus* species with all other *Myxobolus* species was undertaken, as traditional morphological-based myxozoan classification systems are lacking in reliability (Atkinson et al. 2015). The present *Myxobolus* species were considered highly similar to Chinese records describing *Myxobolus physophilus* (Chen 1973; Chen and Ma 1998) in characteristic features of spore morphology (listed in Table 1) and biological traits (host affinity, infection site, and locality). Although the separate morphometrics for smaller and larger polar capsules (length × width) were not given in the former Chinese descriptions (Table 1), the line drawings of spores clearly showed unequal polar capsules (Fig. 3e). Our spore measurements were completed in fresh samples, and thus, these measurements may have been slightly variable than those made in previous Chinese descriptions due to the following reasons: (1)

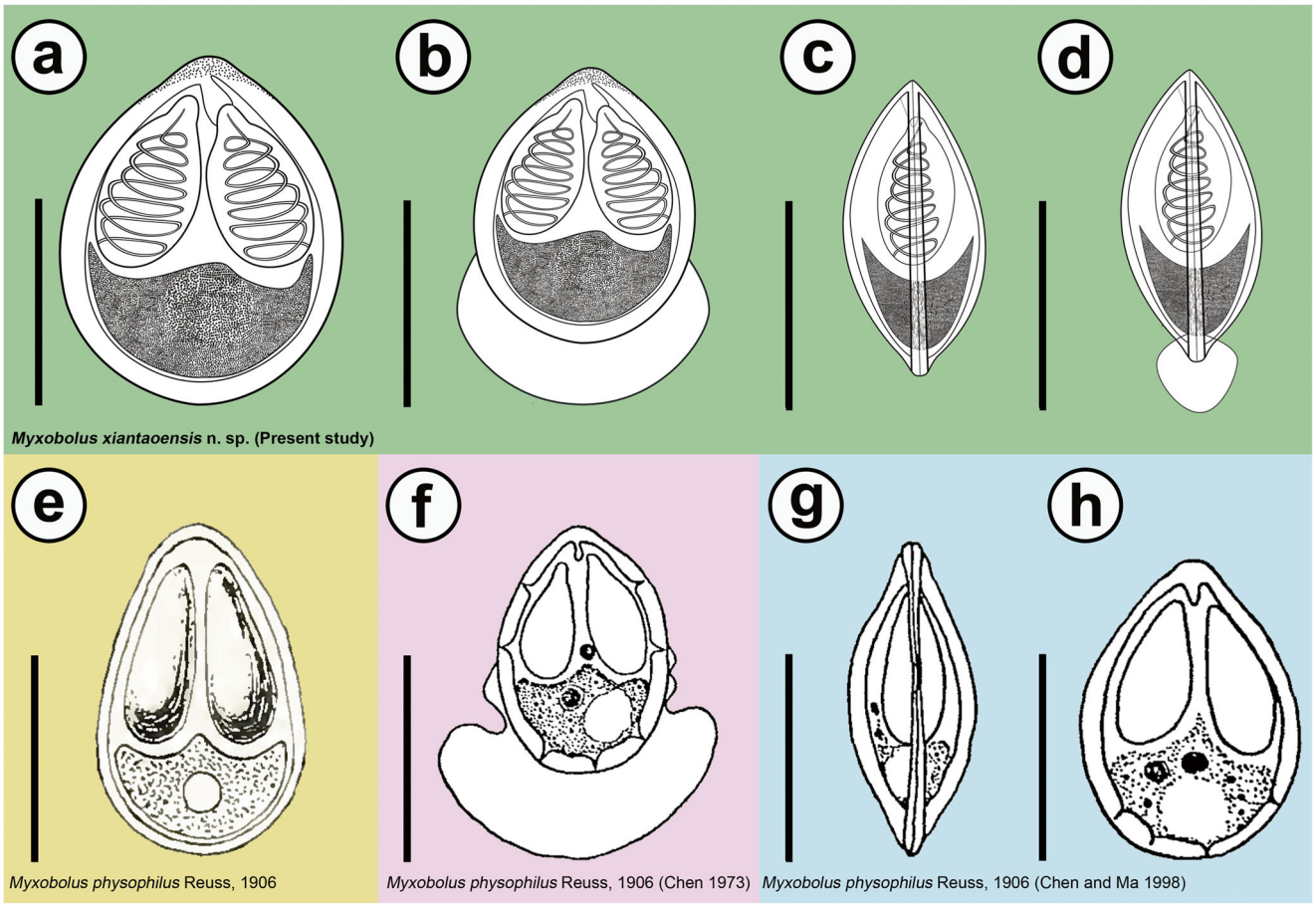

Fig. 3 Diagrammatic illustration of *M. xiantaoensis* n. sp. (**a, b, c, d)** compared with the original description (**e)** and Chinese records (**f, g, h)** of *M. physophilus*. **a** Frontal view without the mucous envelope. Scale bar: 10 μm. **b** Frontal view with the mucous envelope. Scale bar: 10 μm. **c** Sutural view without the mucous envelope. Scale bar: 10 μm. **d** Sutural view with the mucous envelope. Scale bar: 10 μm. **e** Diagrammatic illustration of the original description of *M. physophilus* by Reuss (1906). Scale bar: 10 μm. **f** Frontal view of *M. physophilus* as recorded in China by Chen (1973). Scale bar: 10 μm. **g–h** Sutural and frontal views of *M. physophilus* as recorded in China by Chen and Ma (1998). Scale bar: 10 μm

use of different preparative or (2) difference in morphological methods.

The present *Myxobolus* species and two Chinese records of *M. physophilus* (Fig. 3f–h) differed from the original description of *M. physophilus* (Fig. 3e) in terms of its morphological features, including its spore shape (oval vs. pyriform), intercapsular appendix (absent vs. present), and polar capsule (equal vs. unequal). According to the classification system of Molnár (2002), myxozoans are strictly host/organ/tissue specific. However, both the present *Myxobolus* species and the Chinese records did not correspond well to the original description of *M. physophilus* in terms of either host affinity (*Scardinius erythrophthalmus* vs. *Tachysurus fulvidraco*) and organ affected (air bladder vs. fins). Taken together, these data suggest that Chinese records are easily distinguishable species from the original description of *M. physophilus*. Based on this evidence, we proposed the *Myxobolus* species of present samples and Chinese records of *M. physophilus* from fins of yellow catfish are conspecific and represent a new species, termed *Myxobolus xiantaoensis* n. sp.

Phylogenetic analyses revealed that *M. xiantaoensis* n. sp. was positioned within a mixed clade of *Myxobolus*, *Unicauda*, *Henneguya*, and *Thelohanellus* species (Fig. 5). This tree was largely congruent with previous studies on phylogenetic analyses of genus *Myxobolus* (Eszterbauer 2004; Fiala 2006; Fiala et al. 2015; Holzer et al. 2004; Zhang et al. 2017). Previous studies reported that myxozoan from Cypriniformes fishes (Fiala 2006),

Table 1 Comparative data of *Myxobolus xiantaoensis* n. sp. with former descriptions of *Myxobolus physophilus* and other *Myxobolus* species infecting the fins of Siluriformes

Parasites	Host	Infection site	Location	Intercapsular appendix	Polar filament coils	Spore length × width	Thickness of spore	Polar capsule length × width	Source
Myxobolus xiantaoensis n. sp.	*Tachysurus fulvidraco*	All fins (except adipose fin)	China	Present	6–8	12.6 ± 0.6 (11.3–13.9) × 9.6 ± 0.6 (8.4–11.1)	7.1 ± 0.4 (6.1–7.7)	L*: 6.83 ± 0.5 (8.1–6.0) × 3.4 ± 0.2 (3.8–3.0) S*: 6.4 ± 0.3 (5.5–7.4) × 3.6 ± 0.2 (3.2–3.9)	Present study
M. physophilus, Reuss, 1906 (Chinese record)	*Abbottina rivularis* *Tachysurus nitidus* *Sarcocheilichthys sinensis sinensis* *T. fulvidraco*	Gills, Kidney, urinary bladder, fins	China Russia India	Present	6–7	12.5 (12.0–13.0) × 9.0 (8.4–9.6)	8.4	7.2 (6.6–8.4) × 3.1 (2.8–3.6)	(Chen and Ma 1998)
M. physophilus, Reuss, 1906 (Chinese record)	*T. fulvidraco*	Fins, urinary bladder	China	Present	No data	13.2 (12.6–14.4) × 8.4 (7.2–9.4)	6.0	6.5 (6.0–7.2) × 3.0 (2.6–3.6)	(Chen 1973)
M. physophilus, Reuss, 1906 (original description)	*Scardinius erythrophthalmus*	Surface of air bladder	Russia	Absent	No data	(12–13) × (8.25–9)	(6.5–7)	6 × 2.5	(Kudo 1919, 1933, Reuss 1906)
M. analfnus Basu, Modak & Haldar, 2009	*Heteropneustes fossilis* Bloch, 1794	Anal fin	India	Present	9–10	11.1–13.4 (12.3 ± 0.77) × 7.8–9.3 (8.6 ± 0.42)	6.0–6.5 (6.2 ± 0.53)	L: 3.2–4.9 (4.1 ± 0.4) × 2.0–2.4 (2.2 ± 0.1) S: 2.0–3.1 (2.5 ± 0.3) × 1.6–2.0 (1.8 ± 0.1)	Eiras et al. 2014
M. aureatus Ward, 1919	*T. nitidus* *T. fulvidraco*	Fins, kidney, gallbladder	China	Absent	No data	13.9 (13.7–14.2) × 6.9 (6.8–7.0)	5.6	5.9 (5.8–6.0) × 2.1 (2.1–2.2)	Chen and Ma 1998
M. oviformis Thélohan, 1892	*T. fulvidraco*	Fins, Gill	China, Russia, Germany, France, Switzerland and India	Present	6–7	11.2 (10.8–12.0) × 9.0 (8.4–9.6)	6.3 (6.0–6.6)	5.6 (4.8–6.0) × 2.7 (2.6–2.8)	Chen and Ma 1998
M. ochowensis Chen in Chen & Ma, 1998	*T. fulvidraco*	Dorsal Fins	China	Present	No data	12.8 (12.0–13.2) × 9.5 (8.4–10.2)	7.1 (6.6–7.2)	L: 6.6 (6.0–7.4) × 3.2 (3.0–3.6) S: 6.2 (6.0–6.6) × 2.0 (2.4–3.0)	Chen and Ma 1998
M. huamaensis Liu, 2014	*T. fulvidraco*	Fins	China	Absent	No data	10.3 (9.6–11.0) × 6.8 (6.0–7.2)	No data	3.7 (3.6–3.8) × 2.3 (2.2–2.4)	Liu 2014

*L, larger; *S, smaller; All measurements are in μm, with mean ± standard deviation (if available), and range in parentheses

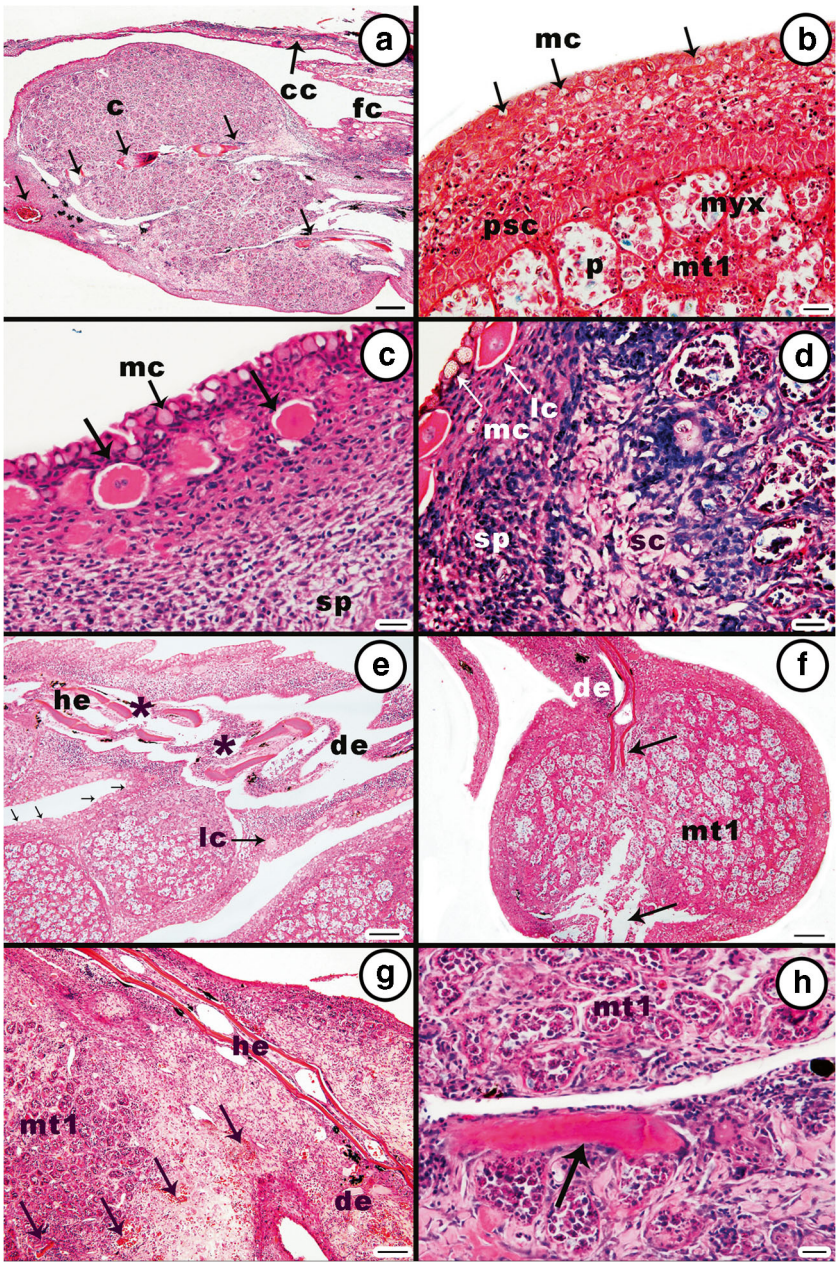

Fig. 4 Histological sections of fins of yellow catfish, affected with *M. xiantaoensis* n. sp. (H & E stain). *Abbreviations*: cc, chondrocytes; c, cysts; fc, fin cartilage; de, deformity; he, hemisegments; lc, leydig cells (alarming cells); mt1, many to one cyst development; mc, mucocytes; myx, myxospores; psc, pseudo stratified columnar cells; p, plasmodia; sp., Stratum spongiosum; sc, Stratum compactum. **a** Fin showing cysts development on the surface of the fin cartilage. *M. xiantaoensis* n. sp. markedly affects the chondrocytes of the fin cartilage. Moreover, cartilaginous islets are present (arrow). Scale bar: 200 μm. **b** Thick outer covering of cysts. Scale bar: 20 μm. **c** Club cells (arrow) and mucous cells in outer layer of cyst. Scale bar: 20 μm. **d** Different layers of cyst wall and small plasmodia containing myxospores. Scale bar: 20 μm. **e** Fin with deformities in hemisegments of fin-ray (*). Scale bar: 100 μm. **f** Fin with breaks in fin-ray (arrow). Scale bar: 100 μm. **g** Fin with broken fragments of fin cartilage (arrow) in the cyst. Scale bar: 100 μm. **h** Cysts containing a fragment of fin cartilage (arrow). Scale bar: 20 μm

Salmoniformes fishes (Ferguson et al. 2008), and Siluriformes fishes (Zhang et al. 2017) tended to form clusters correlating with host affinity. In line with these results, myxozoan species clusters with *M. xiantaoensis* n. sp. infecting Siluriformes fishes from China (predominantly) and Malaysia form a cluster, suggesting that host affinity is a strong phylogenetic signal (Fig. 5).

To conclude, this study underscores the expediency of spore morphology in conjunction with biological traits and phylogenetic analysis in myxozoan characterization. In general, this method must be applied in a systematic way, particularly to differentiate between morphologically described cryptic species or sister-species of myxozoans. In the present work, it allowed a sound integrative taxonomic revision of *M. physophilus* recorded from the fins of yellow catfish in Chinese records as *M. xiantaoensis* n. sp. In Chinese records, beside yellow catfish, *M. physophilus* were also recorded to infect multi-infection sites of the extensively distributed multi-fish hosts based on spore morphology (Table 1). Here, we provide the SSU rDNA sequence of *M. xiantaoensis* n. sp., which will facilitate future work designed to evaluate the validity of *M. physophilus* multi-infection sites of multi-fish host.

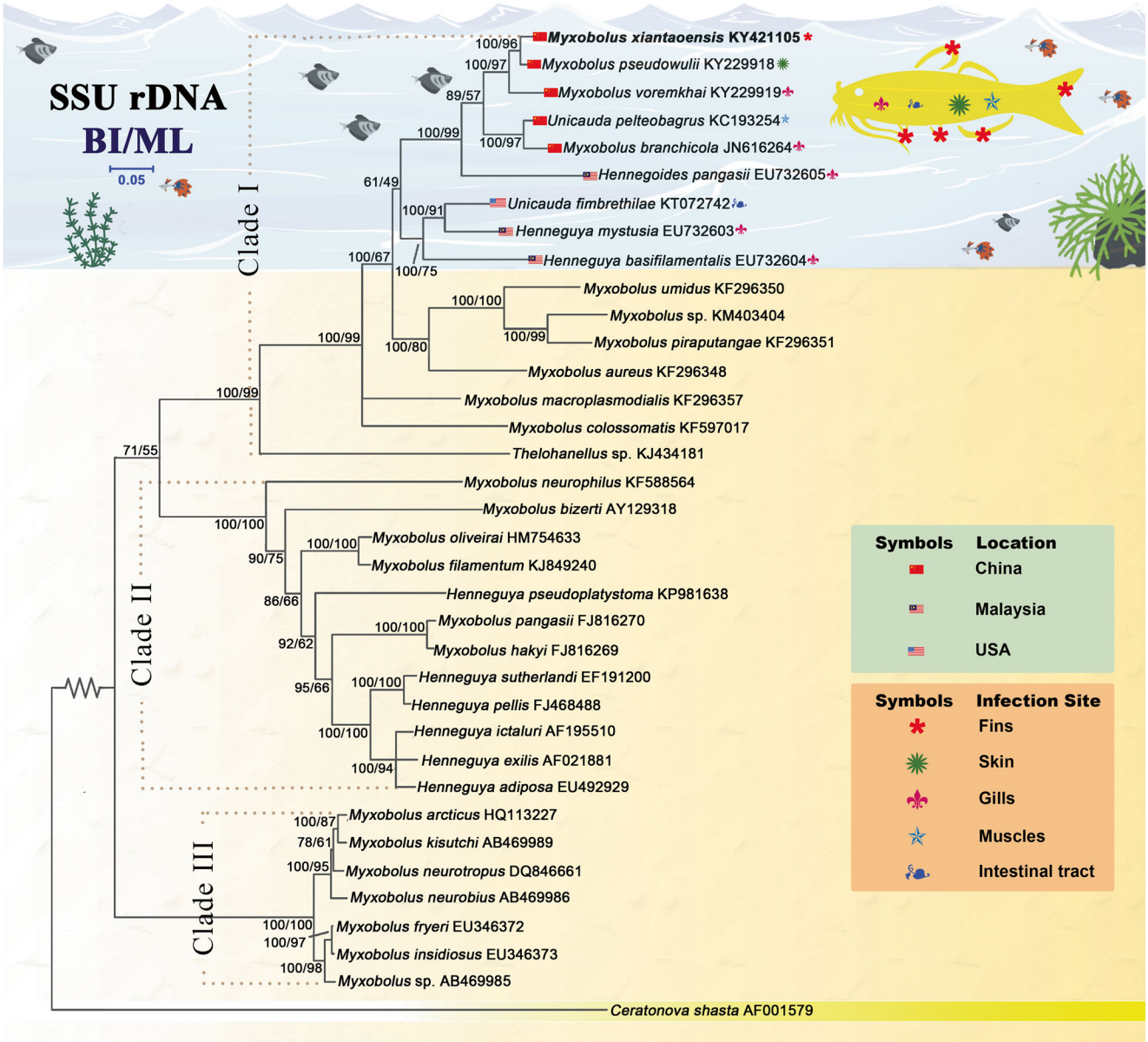

Fig. 5 Phylogenetic analyses made by the BI of aligned partial SSU rDNA sequences of *M. xiantaoensis* n. sp. and related myxosporeans, rooted with *Ceratonova shasta*. GenBank accession numbers are given adjacent to the species names. Numbers given at the nodes of the branches are the posterior probability (BI) and bootstrap (ML) values. The scale bar corresponds to 2 substitutions per 100 nucleotide positions

Funding information This study was supported by the Nature Science Foundation of China (31572233), the China Agriculture Research System (CARS–46), Hubei Agriculture Science and Technology Innovation Center (2016–620–007–001), and the Fundamental Research Funds for the Central Universities (2662015PY089).

Compliance with ethical standards

Ethics approval and consent to participate All animal care protocols complied with the guidelines established by the National Institutes of Health and the International Society for Development Psychobiology (Guide for the care and use of laboratory animals, P 77, Aquatic Animals, National Research Council. 2010).

Consent for publication Not applicable.

Conflict of interest The authors declare that they have no conflicts of interest.

Publisher's note Springer Nature remains neutral with regard to jurisdictional claims in published maps and institutional affiliations.

References

Abdel-Ghaffar F, Abdel-Baki AA, Garhy ME (2005) Ultrastructural characteristics of the sporogenesis of genus *Myxobolus* infecting some Nile fishes in Egypt. Parasitol Res 95:167–171. https://doi.org/10.1007/s00436-004-1250-1

Atkinson SD, Bartošová-Sojková P, Whipps CM, Bartholomew JL (2015) Approaches for characterising Myxozoan species. In:

Myxozoan evolution, ecology and development. Springer International Publishing Cham, Basel, pp 111–123. https://doi.org/10.1007/978-3-319-14753-6_6

Chen C (1973) Classification of pathogens. Illustration of fish pathogens in Hubei Province. Science Press, Beijing

Chen QL, Ma CL (1998) Fauna Sinica: Myxozoa, Myxosporea. Science Press, Beijing

Eiras J, Molnár K, Lu Y (2005) Synopsis of the species of *Myxobolus* Bütschli, 1882 (Myxozoa: Myxosporea: Myxobolidae). Syst Parasitol 61:1–46. https://doi.org/10.1007/s11230-004-6343-9

Eiras JC, Zhang J, Molnár K (2014) Synopsis of the species of *Myxobolus* Bütschli, 1882 (Myxozoa: Myxosporea, Myxobolidae) described between 2005 and 2013. Syst Parasitol 88:11–36. https://doi.org/10.1007/s11230-014-9484-5

Eszterbauer E (2004) Genetic relationship among gill-infecting *Myxobolus* species (Myxosporea) of cyprinids: molecular evidence of importance of tissue-specificity. Dis Aquat Org 58:35–40. https://doi.org/10.3354/dao058035

Ferguson JA, Atkinson SD, Whipps CM, Kent ML (2008) Molecular and morphological analysis of *Myxobolus* spp. of salmonid fishes with the description of a new *Myxobolus* species. J Parasitol 94:1322–1334. https://doi.org/10.1645/GE-1606.1

Fiala I (2006) The phylogeny of Myxosporea (Myxozoa) based on small subunit ribosomal RNA gene analysis. Int J Parasitol 36:1521–1534. https://doi.org/10.1016/j.ijpara.2006.06.016

Fiala I, Bartošová-Sojková P, Whipps CM (2015) Classification and phylogenetics of Myxozoa. In: Myxozoan evolution, ecology and development. Springer nternational Publishing Cham, Basel, pp 85–110. https://doi.org/10.1007/978-3-319-14753-6_5

Forró B, Eszterbauer E (2016) Correlation between host specificity and genetic diversity for the muscle-dwelling fish parasite *Myxobolus pseudodispar*: examples of myxozoan host–shift? Folia Parasitol 63(019). https://doi.org/10.14411/fp.2016.019

Guindon S, Dufayard J–F, Lefort V, Anisimova M, Hordijk W, Gascuel O (2010) New algorithms and methods to estimate maximum–likelihood phylogenies: assessing the performance of PhyML 3.0. Syst Biol 59:307–321. https://doi.org/10.1093/sysbio/syq010

Hall TA (1999) BioEdit: a user-friendly biological sequence alignment editor and analysis program for windows 95/98/NT. Nucleic Acids Symp Ser 41:95–98

Heiniger H, Adlard RA (2013) Molecular identification of cryptic species of *Ceratomyxa Thélohan*, 1892 (Myxosporea: Bivalvulida) including the description of eight novel species from apogonid fishes (Perciformes: Apogonidae) from Australian waters. Acta Parasitol 58:342–360

Hillis DM, Dixon MT (1991) Ribosomal DNA: molecular evolution and phylogenetic inference. Inference Q Rev Biol 66:411–453

Holzer AS, Sommerville C, Wootten R (2004) Molecular relationships and phylogeny in a community of myxosporeans and actinosporeans based on their 18S rDNA sequences. Int J Parasitol 34:1099–1111. https://doi.org/10.1016/j.ijpara.2004.06.002

Katoh K, Standley DM (2013) MAFFT multiple sequence alignment software version 7: improvements in performance and usability. Mol Biol Evol 30:772–780. https://doi.org/10.1093/molbev/mst010

Kudo R (1919) Illinois biological monographs. In: Forbes SA, Trelease W, Ward HB (eds). Published quarterly under the auspices of the graduate school by the University of Illinois, Urbana, Illinois, p 155

Kudo R (1933) A taxonomic consideration of Myxosporidia. Trans Am Microsc Soc 52:195–216

Liu S (1997) A study on the biology of *Pseudobagrus fulvidrac*o in poyanglake. Chin J Zool 32:10–16

Liu Y (2014) Revision on genus *Myxobolus* (Myxozoa: Myxosporea) and taxonomy of some *Myxobolus* species in China. Ph.D. dissertation submitted in Huazhong Agricultural University, Wuhan, P.R. China

Liu Y, Whipps CM, Nie P, Gu Z (2014) *Myxobolus oralis* n. sp. (Myxosporea: Bivalvulida) infecting the palate in the mouth of gibel carp *Carassius auratus* gibelio (Cypriniformes: Cyprinidae). Folia Parasitol 61:505–511. https://doi.org/10.14411/fp.2014.052

Liu Y, Zhai Y, Gu Z (2016) Morphological and molecular characterization of *Thelohanellus macrovacuolaris* n. sp. (Myxosporea: Bivalvulida) infecting the palate in the mouth of common carp *Cyprinus carpio* L. in China. Parasitol Int 65:303–307. https://doi.org/10.1016/j.parint.2016.02.013

Lom J, Dyková I (1992) Protozoan parasites of fishes, developments in aquaculture and fisheries science. Elsevier, Amsterdam

Lom J, Dyková I (2006) Myxozoan genera: definition and notes on taxonomy, life-cycle terminology and pathogenic species. Folia Parasitol 53:1–6

Molnár K (1994) Comments on the host, organ and tissue specificity of fish myxosporeans and on the types of their intrapiscine development. Parasitol Hung 27:5–20

Molnár K (2002) Site preference of myxosporean spp. on the fins of some Hungarian fish species. Dis Aquat Org 48:123–128. https://doi.org/10.3354/dao052123

Molnár K, Eszterbauer E (2015) Specificity of infection sites in vertebrate hosts. In: Myxozoan evolution, ecology and development. Springer International Publishing Cham, Basel, pp 295–313. https://doi.org/10.1007/978-3-319-14753-6_16

Molnár K, Székely C, Hallett SL, Atkinson SD (2009) Some remarks on the occurrence, host-specificity and validity of *Myxobolus rotundus* Nemeczek, 1911 (Myxozoa: Myxosporea). Syst Parasitol 72:71–79. https://doi.org/10.1007/s11230-008-9161-7

Naldoni J, Zatti SA, Capodifoglio KR, Milanin T, Maia AA, Silva MR, Adriano EA (2015) Host-parasite and phylogenetic relationships of *Myxobolus filamentum* n. sp. (Myxozoa: Myxosporea), a parasite of *Brycon orthotaenia* (Characiformes: Bryconidae) in Brazil. Folia Parasitol 62(1). https://doi.org/10.14411/fp.2015.014

Nylander J (2004) MrModeltest v2 (Program distributed by the author, Evolutionary Biology Centre, Uppsala University, Uppsala, Sweden)

Okamura B, Gruhl A, Bartholomew JL (2015) Myxozoan evolution, ecology and development. Springer International Publishing, Cham

Reuss H (1906) Neue Myxosporidien von Siisswasserfischen, Bulletin de l'Académie impériale des sciences de St.–Pétersbourg, pp 201–202. (In Russian)

Ronquist F, Huelsenbeck JP (2003) MrBayes 3: Bayesian phylogenetic inference under mixed models. Bioinformatics 19:1572–1574

Székely C, Molnár K (1999) *Myxobolus* infection of the gills of common bream (*Abramis brama* L.) in Lake Balaton and in the Kis-Balaton reservoir, Hungary. Acta Vet Hung 47:419–432. https://doi.org/10.1556/AVet.47.1999.4.3

Székely C, Molnár K, Cech G (2015) Description of *Myxobolus balatonicus* n. sp. (Myxozoa: Myxobolidae) from the common carp *Cyprinus carpio* L. in Lake Balaton. Syst Parasitol 91:71–79. https://doi.org/10.1007/s11230-015-9560-5

Tamura K, Stecher G, Peterson D, Filipski A, Kumar S (2013) MEGA6: molecular evolutionary genetics analysis version 6.0. Mol Biol Evol 30:2725–2729. https://doi.org/10.1093/molbev/mst197

Whipps CM, Adlard RD, Bryant MS, Lester RJ, FINDLAV VKML (2003) First report of three *Kudoa* species from eastern Australia: *Kudoa thyrsites* from mahi mahi (*Coryphaena hippurus*), *Kudoa amamiensis* and *Kudoa minithyrsites* n. sp. from sweeper (*Pempheris ypsilychnus*). J Eukaryot Microbiol 50:215–219. https://doi.org/10.1111/j.1550-7408.2003.tb00120.x

Yuan X, Zhao W (2016) China fishery statistics yearbook 2016. China Agriculture Press, Beijing

Zhang B, Zhai Y, Liu Y, Gu Z (2017) *Myxobolus pseudowulii* n. sp. (Myxozoa: Myxosporea), a new skin parasite of yellow catfish *Tachysurus fulvidraco* (Richardson) and redescription of *Myxobolus voremkhai* (Akhmerov, 1960). Folia Parasitol 64. https://doi.org/10.14411/fp.2017.030